Available online at www.sciencedirect.com

SCIENCE DIRECT®

Journal of Organometallic Chemistry 691 (2006) 1934–1940

Journal of Organo metallic Chemistry

www.elsevier.com/locate/jorganchem

Reactions of pentaborane(9) with electron-rich molybdenum and tungsten phosphine polyhydrides

Malcolm L.H. Green [a], J. Walker [a], P. Mountford [a], John B. Leach [b], Malcolm A. Kelland [c,*]

[a] Inorganic Chemistry Laboratory, South Parks Road, Oxford OX1 3QR, UK
[b] Department of Chemistry, Manchester Metropolitan University, John Dalton Building, Chester Street, Manchester M1 5GD, UK
[c] Department of Science and Technology, University of Stavanger, Kristine Bonnevies vei 1, P.O. Box 8002, N-4036 Stavanger, Norway

Received 28 November 2005; received in revised form 4 January 2006; accepted 5 January 2006
Available online 14 February 2006

Abstract

Reaction of $[W(PMe_2Ph)_3H_6]$ with pentaborane(9) gives *nido*-2-$[W(PMe_2Ph)_3H_2B_4H_8]$ (**1**) as well as *nido*-2-$[W(PMe_2Ph)_3HB_5H_{10}]$ (**2**). The crystal structure of (**2**) has been determined. Compound (**2**) has a novel metallaborane structure containing an edge-bridging $\{BH_3\}$ group between the tungsten atom and one of the basal boron atoms in a "*nido*-WB_4" pyramid. Reaction of $[W(PMe_3)_4(\eta^2\text{-}CH_2PMe_2)H]$ with pentaborane(9) gives *nido*-2-$[W(PMe_3)_3H_2B_4H_8]$ (**3**) whilst reaction of $[Mo(L)_4H_4]$ with pentaborane(9) gives *nido*-2-$[Mo(L)_3H_2B_4H_8]$ [L = PMe_3 (**4**), PMe_2Ph (**5**)]. Treatment of $[Mo(PMe_3)_4H_4]$ with excess $BH_3 \cdot$ thf gives the known borohydride $[Mo(PMe_3)_4H(\eta^2\text{-}BH_4)]$.

© 2006 Elsevier B.V. All rights reserved.

Keywords: Boron hydrides; Pentaborane(9); Metallaboranes; Molybdenum; Tungsten; Crystal structure

---

1. Introduction

The reaction of pentaborane(9) (*nido*-B_5H_9) with transition-metal compounds or the $[nido - B_5H_8^-]$ anion with transition-metal chlorides gives a wide variety of metallaborane structures [1–4]. We are exploring the reaction of pentaborane(9) with electron-rich transition-metal compounds. For example, the reaction of pentaborane(9) with $[Fe(PMe_3)_3(\eta^2\text{-}CH_2PMe_2)H]$ gives the novel borane-capped *nido*-ferrapentaborane $[2,3\text{-}\{Fe(PMe_3)_2\}_2(\eta\text{-}H)B_4H_9]$ and nido-2-$[Fe(PMe_3)_3B_4H_8]$ [5]. Further, the reaction of $[(\eta\text{-}C_5Me_5)Ru(PMe_3)H_3]$ with pentaborane(9) gives several metallaboranes with 3–5 boron atoms including *nido*-2-$[(\eta\text{-}C_5Me_5)RuB_5H_{10}]$, *arachno*-2-$[(\eta\text{-}C_5Me_5)Ru(PMe_3)B_3H_8]$, *arachno*-3-$[(\eta\text{-}C_5Me_5)Ru(PMe_3)B_4H_9]$ and *nido*-2-$[(\eta\text{-}C_5Me_5)(PMe_3)RuB_5H_8]$ [6]. We have also reported the reaction of the tungsten complex $[W(PMe_3)_3H_6]$ with metallaboranes to give novel metallaborane clusters [7,8]. We decided to extend the study to the reaction of pentaborane(9) with electron-rich phosphine polyhydrides of tungsten and molybdenum. Only two previous studies of the reaction of Group 6 electron-rich phosphine polyhydrides with boron hydrides have been reported. $[W(PMe_3)_3H_6]$ reacts with $BH_3 \cdot$ thf to give *arachno*-2-$[W(PMe_3)_3H_3B_3H_8]$ [9] whilst reaction of $[W(PMe_2Ph)_3H_6]$ with $[NEt_4][B_9H_{14}]$ gives *nido*-$[W(PMe_2Ph)_3H_2B_9H_{13}]$ [10].

2. Results and discussion

Treatment of a toluene solution of $[W(PMe_2Ph)_3H_6]$ [18] with excess of a toluene solution of pentaborane(9) gave a red–brown solution from which two products could be separated in low yields by column chromatography on silica gel. Light petroleum ether:thf 20:1 eluted *nido*-2-$[W(PMe_2Ph)_3H_2B_4H_8]$ (**1**) as a bright yellow band. Light petroleum ether:thf 9:1 eluted $[W(PMe_2Ph)_3HB_5H_{10}]$ (**2**) as a dark orange–brown band. Recrystallisation of the yellow band from light petroleum ether afforded yellow microcrystals of (**1**). Recrystallisation of the orange–brown

---

[*] Corresponding author. Tel.: +47 51831823; fax: +47 51831750.
E-mail address: malcolm.kelland@uis.no (M.A. Kelland).

0022-328X/$ - see front matter © 2006 Elsevier B.V. All rights reserved.
doi:10.1016/j.jorganchem.2006.01.006

band from light petroleum ether afforded purple microcrystals of (**2**).

Compound (**1**) has been characterised by multi-nuclear NMR spectroscopy and elemental analysis as *nido*-2-[$W(PMe_2Ph)_3H_2B_4H_8$] (Fig. 1). The metallaborane "MB_4H_8" cage in (**1**) is known for a number of transition metals including tantalum [11], tungsten [7,12,25], iron [6] and cobalt [13]. The ^{11}B NMR spectrum of (**1**) consists of three resonances of relative intensity 1:2:1. Both the low field and high field resonances are resolved as doublets whilst the resonance in-between is broad and unresolved. $^{11}B\{^1H\}$ broad band decoupling of these signals collapses the doublets to singlets and the broad resonance to sharpen considerably to a singlet. The ^1H NMR of (**1**) shows five resonances that sharpen on broad band ^{11}B decoupling. These can be definitively assigned by $^1H\{^{11}B\}$ and $^{11}B\{^1H\}$ selective decoupling experiments as two equivalent W–H–B bridging protons, two equivalent B–H–B bridging protons and four terminal B–H protons two of which are equivalent. Also present in the ^1H NMR spectrum are signals due to the three dimethylphenylphosphine ligands and the two hydrides on the tungsten. Spin saturation transfer experiments performed on (**1**) show exchange between the W–H–B bridges and the W–H hydrides at room temperature.

Compound (**2**) has been characterised by multi-nuclear NMR spectroscopy, mass spectroscopy, elemental analysis and X-ray crystallography. The complexity of the NMR data were sufficient to warrant a structural investigation. Purple needles of (**2**) suitable for X-ray diffraction were grown from toluene:light petroleum ether. Crystallographic data are collected in Table 1. A selected view of the molecular structure of (**2**) is given in Fig. 2 and selected bond lengths in Table 2.

The X-ray diffraction study revealed a structure based on a *nido*-pentaborane(9) cluster with the $\{W(PMe_2Ph)_3H\}$ fragment subrogating for a basal boron unit as in compound (**1**). The most surprising feature of the structure is the presence of an edge-bridging $\{BH_3\}$ unit [atom B(6)] which substitutes for one of the bridge hydrogen atoms between the metal and one of the basal boron atoms B(5). One of the hydrogen atoms on this $\{BH_3\}$ unit is bridging between (B6) and the metal, with the other two terminal hydrogen atoms *exo* and *endo* on this boron.

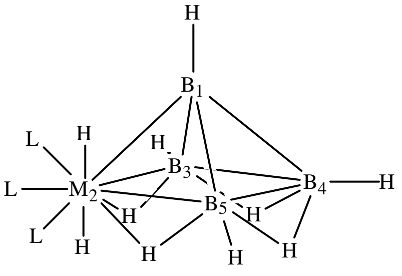

Fig. 1. Structures of *nido*-2-[$M(L)_3H_2B_4H_8$]. M = W, L = PMe_2Ph (**1**); M = W, L = PMe_3 (**3**); M = Mo, L = PMe_2Ph (**4**); M = Mo, L = PMe_3 (**5**).

Table 1
Crystal data, data collection and structure refinement for *nido*-2-[$W(PMe_2Ph)_3HB_5H_{10}$] (**2**)

Empirical formula	$C_{24}H_{44}B_5P_3W$
Molecular weight	663.4
Crystal size (mm)	0.1 × 0.3 × 0.3
Crystal system	Monoclinic
Space group	$P2_1/c$
a (Å)	14.752(8)
b (Å)	22.805(6)
c (Å)	10.103(3)
β (°)	98.09
Volume (Å^3)	3364.9
Z	4
D_c (g cm^{-3})	1.31
μ (cm^{-1})	36.6
$F(000)$	1328
T (K)	293 (10)
Radiation (λ/μ) Mo Kα	(0.71069)
2θ Limits (°)	3–48
Scan mode	ω-2θ
Total data collected	5266
Number of observations	3160
Number of variables	341
Observations/variables	9.27
Weighting scheme	Unit weights
R	0.0391
R_w	0.0432

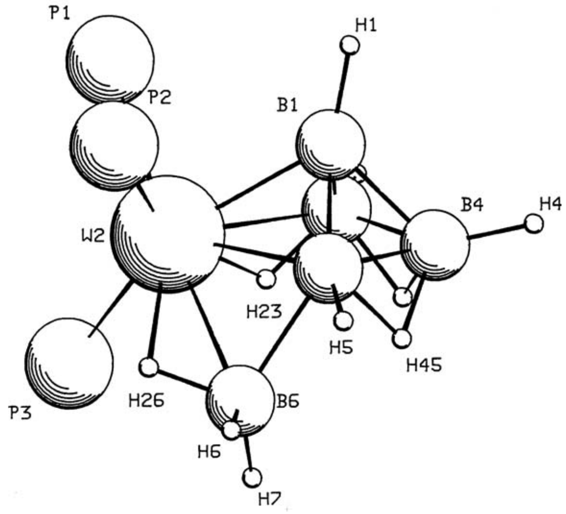

Fig. 2. Molecular structure of *nido*-2-[$W(PMe_2Ph)_3HB_5H_{10}$] (**2**). The methyl and phenyl groups on the phosphine ligands have been omitted for clarity. The W–H hydrogen atom is not shown.

There are several bond lengths of note in the structure of (**2**). The W–H–B distance from the metal fragment to the $\{BH_3\}$ unit is relatively short (2.363 Å). Otherwise the other W–B distances within the square pyramid compare well with previously reported nido-"MB_4H_8" metallaboranes such as [$Cp^*WH_3B_4H_8$] [12], [$Cp^*TaCl_2B_4H_8$] [11] and [$CpCoB_4H_8$] [13]. The corresponding B(5)–B(6) bond to the $\{BH_3\}$ unit appears to be marginally longer (1.88 Å) than the bridged B–B bonds (1.78, 1.83 Å) in the same structure. The other B–B, W–B and W–P bond

Table 2
Selected bond distances and angles for compound (**2**)

Bond distances	
W(2)–B(1)	2.231(12)
W(2)–B(3)	2.426(13)[a]
W(2)–B(5)	2.328(12)
W(2)–B(6)	2.363(13)[a]
W(2)–P(1)	2.505(2)
W(2)–P(2)	2.450(2)
W(2)–P(3)	2.500(2)
B(1)–B(3)	1.69(2)
B(1)–B(4)	1.74(2)
B(1)–B(5)	1.75(2)
B(3)–B(4)	1.78(2)
B(4)–B(5)	1.83(2)
B(5)–B(6)	1.88(3)
Bond angles	
B(1)–W(2)–B(3)	42.39
B(1)–W(2)–B(5)	45.20
B(3)–W(2)–B(5)	66.92
B(3)–B(4)–B(5)	93.15
W(2)–B(6)–B(5)	65.27
W(2)–B(3)–B(4)	98.94
B(3)–B(1)–B(4)	62.35
W(2)–B(1)–B(3)	75.03
B(1)–B(3)–B(4)	60.03

[a] Bonds which have bridging hydrogen atoms.

lengths are comparable to those in other tungstenaboranes [9,10,12].

The ^{11}B NMR spectrum of (**2**) consists of five resonances of relative intensity 1:1:1:1:1. The four higher field resonances resolve into doublets whereas the lower field resonance ($\delta = 32.0$ ppm) appears as a very broad triplet. Assignments of the boron and proton nuclei in (**2**) were made using $^{1}\mathrm{H}\{^{11}\mathrm{B}\}$ and $^{11}\mathrm{B}\{^{1}\mathrm{H}\}$ selective decoupling experiments as well as ^{11}B–^{11}B COSY and ^{1}H–^{11}B shift correlation experiments. An unusual feature of the ^{11}B NMR spectrum is the position of the apex boron (B1) which is found in the middle of the resonances resulting from the basal boron atoms at $\delta = 6.83$ ppm. A typical apex boron would be expected to appear at $\delta = -30$ to -50 ppm in *nido*-$\{MB_4H_8\}$ clusters and is usually found at the highest field position in the ^{11}B NMR spectrum. The edge-bridging boron atom B(6) is found at low field ($\delta = 32.0$ ppm) and shows no correlation with any of the other boron atoms in the ^{11}B–^{11}B COSY spectrum, although one would have expected to see the correlation to the unbridged boron B(5). This may be the result of the very broad nature of the B(6) resonance. The correlation of the proposed apical boron B(1) to B(3), B(4), and B(5) is clearly seen in the ^{11}B–^{11}B COSY spectrum. In the ^{1}H–^{11}B shift correlation spectrum only the proton (H34) was found not to correlate to its attached boron nucleus B(3), although it showed a strong correlation to the other attached boron B(4). Otherwise each boron nuclei correlated correctly to its respective terminal proton and bridge protons where appropriate. B(6) showed correlations only with its W–H–B bridge.

The $^{1}\mathrm{H}\{^{11}\mathrm{B}\}$ NMR spectrum revealed 9 different resonances for the $\{WB_5H_{10}\}$ cluster fragment, eight of relative intensity one and one of intensity 2 for protons H(6) and H(7) which were not resolved. An unusual feature of the ^{1}H NMR spectrum is the location of the apical terminal proton which is found at a much lower field ($\delta = 3.1$ ppm) than usually expected (corresponding to the low field position of the apical boron in the ^{11}B NMR spectrum). The single tungsten hydride is observed as a broad multiplet at $\delta = -0.3$ ppm. The ^{31}P NMR spectrum for (**2**) consists of two signals, a doublet ($\delta = -16.67$ ppm, 2P) and a triplet ($\delta = -29.28$ ppm, 1P).

From the electron-counting rules for clusters [14–16], one would predict a structure based on the parent neutral borane *nido*-$[B_6H_{10}]$ (16 cluster electrons). The geometry observed for compound (**2**) does not resemble *nido*-$[B_6H_{10}]$ rather the presence of the bridging {3} unit indicates closer similarities with the proposed structure for the *arachno*-$[B_6H_{11}^-]$ ion (Fig. 3). In addition, there are many six-vertex metallaborane analogues which are bridge-substituted pentaboranyl metal derivatives which can also be considered as having a gross geometry similar to that proposed for the *arachno*-$[B_6H_{11}^-]$ ion [2,3]. In these examples however, the metal fragment substitutes for one of the bridge hydrogen atoms, whereas in (**2**) the metal fragment is retained in a basal boron position and a boron atom is substituted in the bridge hydrogen position.

It may be best to consider compound (**2**) as a substituted version of compound (**1**). In going from (**1**) to (**2**) a W–H–B bridging hydrogen atom has been replaced by a $\{BH_2\}$ unit which interacts with one of the W–H hydrides (to enable the boron to fill its octet) to produce a bridge to the metal. The bonding characteristics of a $\{BH_2\}$ unit and a hydrogen atom can be seen to be similar in the valence bond structure. This similarity has been used to describe the structural relationship between the *arachno*-boranes $[B_4H_{10}]$, $[B_5H_{11}]$ and $[B_6H_{12}]$ [17]. The structure of $[B_5H_{11}]$ can be derived from $[B_4H_{10}]$ by replacing one of the B–H–B bridging hydrogens with a $\{BH_2\}$ unit and, at the same time, allowing one of the terminal hydrogens adjacent to the substitution to now become bridging to the $\{BH_2\}$ unit (Fig. 4).

If the same procedure is performed on *nido*-$[B_5H_9]$ we obtain *nido*-$[B_6H_{10}]$, but the geometry observed will not look like that of the known structure which is pentagonal pyramidal (Fig. 5).

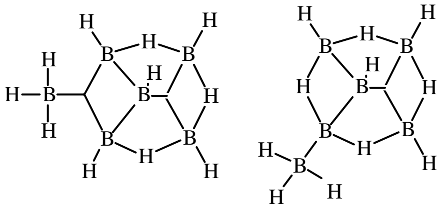

Fig. 3. Two possible valence bond structures for the *arachno*-$[B_6H_{11}^-]$ ion.

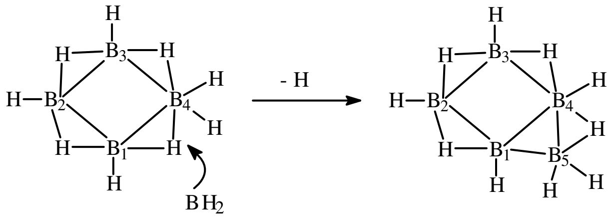

Fig. 4. Relationship between $[B_4H_{10}]$ and $[B_5H_{11}]$.

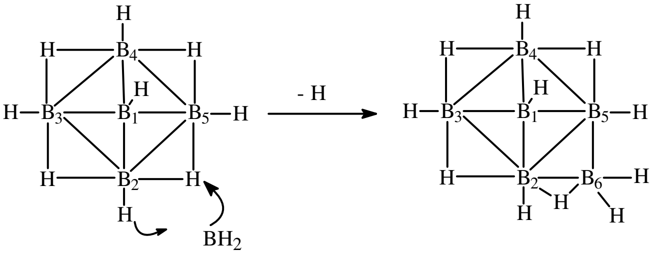

Fig. 5. Relationship between $[B_5H_9]$ and $[B_6H_{10}]$.

Although the stoichiometry is $[B_6H_{10}]$, what we actually observe is a structure which resembles that of the structure proposed for *arachno*-$[B_6H_{11}^-]$. The schematic representation in Fig. 5 would result in one of the boron atoms adjacent to the $\{BH_2\}$ unit, B(2), not having a terminal hydrogen attached to it. In electron-counting in this cluster the two electrons it would have had involved in this bonding interaction should be considered to contribute to the skeletal framework. Thus, this boron atom will now contribute 3 electrons and 4 orbitals to the cluster count. The cluster count is as follows: $4 \times (BH = 2) = 8e$, $1 \times (BH_2) = 3e$, $1B = 3e$, $4 \times (\mu\text{-H}) = 4e$, this is a total of 18e or 9 electron pairs. This gives us a $n + 3$ arachno cluster for six skeletal atoms. This indicates a structure based on that proposed for the *arachno*-$[B_6H_{11}^-]$ ion as suggested earlier.

We can also suggest that the same relationship exists between the structures of compounds (**1**) and (**2**). The metal fragment $\{W(PMe_2Ph)_3H_2\}$ in (**1**) can be considered as the $\{BH\}$ fragment of the $[B_5H_9]$ cage. Thus, it is possible to envisage substitution of the bridging hydrogen atom adjacent to the metal by a $\{BH_2\}$ unit, simultaneously followed by the tungsten hydride forming the bridge to this unit (Fig. 6). The remaining $\{W(PMe_2Ph)_3H\}$ moiety behaves as the boron atom with no terminal hydrogen and contributes 3 electrons to the cluster. Thus, the overall cluster count is the same as before, 18 electrons, to give the analogous $n + 3$ condition which is a structure based on the *arachno*-$[B_6H_{11}^-]$ ion. This is indeed the X-ray diffraction structure observed.

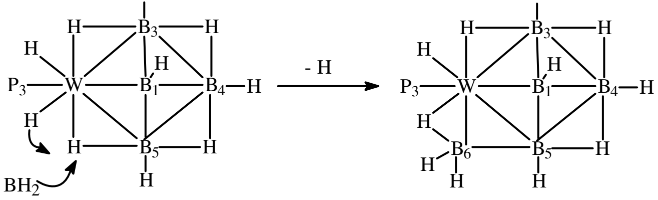

Fig. 6. Relationship between *nido*-2-$[W(PMe_2Ph)_3H_2B_4H_8]$ (**1**) and *nido*-2-$[W(PMe_2Ph)_3HB_5H_{10}]$ (**2**).

Reaction of $[W(PMe_3)_4(\eta^2\text{-}CH_2PMe_2)H]$ [19] with pentaborane(9) gives *nido*-2-$[W(PMe_3)_3H_2B_4H_8]$ (**3**) after work-up by column chromatography (Fig. 1). Compound (**3**) has been characterised by elemental analysis and multi-nuclear NMR using selective $^1H\{^{11}B\}$ decoupling experiments to assign the protons. As expected, the NMR spectra of (**3**) show strong similarities to compound (**1**) and to *nido*-2-$W(PMe_3)_3H_2B_4H_7[Mo(\eta\text{-}C_5H_5)(\eta^5\text{:}\eta^1\text{-}C_5H_4)H_2]$ which we recently reported [7]. This latter molecule contains the same *nido*-"WB_4" cage as in (**3**) as well as the same phosphine ligands on the tungsten fragment. A minor purple product from the reaction of $[W(PMe_3)_4(\eta^2\text{-}CH_2PMe_2)H]$ with pentaborane(9) was studied by NMR spectroscopy. It was not isolated in pure form but gave similar shielding patterns as for compound (**2**) and is probably the PMe_3 analogue of compound (**2**).

To extend the study to metallaboranes of molybdenum we sought $[Mo(L_3)H_6]$ polyhydrides of molybdenum. These are less accessible than the tungsten analogues and are unknown for $L = PMe_3$ and PMe_2Ph. Therefore, we used the easily synthesised tetrahydrides $[Mo(L)_4H_4]$ [20].

Reaction of $[Mo(L)_4H_4]$ with pentaborane(9) gives *nido*-2-$[Mo(L)_3H_2B_4H_8]$ [$L = PMe_3$ (**4**), PMe_2Ph (**5**)] (Fig. 1). Reaction of $[Mo(PEtPh_2)_4H_4]$ with pentaborane(9) gave no metallaborane products even after prolonged heating to 60 °C. Compounds (**4**) and (**5**) have been characterised by elemental analysis and multi-nuclear NMR.

The solution $^1H\{^{11}B\}$, ^{11}B and $^{31}P\{^1H\}$ NMR spectra of (**4**) were found to be very similar to the tungsten analogue (**3**) from which we deduce the proposed structure *nido*-2-$[Mo(PMe_3)_3H_2B_4H_8]$ (Fig. 1). For example, the ^{11}B NMR spectrum of (**4**) shows resonances at $\delta = -2.6$ (1B), -7.3 (2B) and -27.2 ppm (1B) compared to $\delta = -3.7$ (1B), -9.7 (2B) and -29.7 ppm (1B) for the tungsten cluster. The $^1H\{^{11}B\}$ NMR spectrum of (4) shows five resonances (ratio 1:2:1:2:2) assigned to the hydrogens associated with the $\{B_4H_8\}$ fragment, as well as a quartet at $\delta = -4.53$ ppm assigned to 2 Mo–H hydrogens and a virtual triplet at $\delta = 1.23$ ppm assigned to the three PMe_3 ligands. The skeletal electron count for the molecule is seven pairs, which fits the requirements for a square pyramidal geometry.

The minor purple fraction (**6**) separated by column chromatography from the reaction of pentaborane(9) with $[Mo(PMe_3)_3H_4]$ was studied by multi-nuclear NMR spectroscopy and found to be thermally unstable. Several attempts to obtain a clean sample for complete NMR characterisation, either by low temperature NMR spectroscopy and/or low temperature recrystallisations failed. However, it was possible to make some inferences from the spectra of impure samples. The $^{11}B\{^1H\}$ NMR spectrum showed 5 major resonances in 1:1:1:1:1 ratio. The ^{11}B NMR spectrum and high field region of the ^{1}H NMR spectrum of (**6**) show close similarities in their shielding patterns with that of purple (**2**). In particular, and as found for compound (**2**), the low field resonance was resolved as a broad triplet indicating two terminal hydrogen atoms on this boron atom. Assignments of the B–H terminal protons in the low field region of the $^{1}H\{^{11}B\}$ NMR spectrum were not obtained. However, from the partial data obtained it seems likely that (**6**) is the $\{BH_3\}$ edge-substituted metallaborane *nido*-2-$[Mo(PMe_3)_3HB_5H_{10}]$ (Fig. 7).

The reaction of pentaborane(9) with $[Mo(PMe_2Ph)_3H_4]$ occurs much more slowly than with $[Mo(PMe_3)_3H_4]$ to give a mixture of products from which only low yields of red *nido*-2-$[Mo(PMe_2Ph)_3H_2B_4H_8]$ (**5**) could be isolated by column chromatography (Fig. 1). The positioning and pattern of the cluster resonances in the $^{1}H\{^{11}B\}$, ^{11}B and $^{31}P\{^{1}H\}$ NMR spectra are very similar to those of compound (**4**). The resonances in the ^{11}B NMR spectrum of (**5**) are broader than those of (**4**) and show less doublet resolution associated with B–H terminal coupling. It is not clear whether this is due to the relative electron-donating abilities of the phosphines or a relaxation effect due to the bulk of the ligands.

Transition metal hydrides have also been shown to react with $BH_3 \cdot$ thf. For example, Fehlner and co-workers have also reported the reaction of $BH_3 \cdot$ thf with transition metal hydrides. $[Fe(\eta\text{-}C_5Me_5)H_2]_2$ gives the monometal cluster *arachno*-1-$[Fe(\eta\text{-}C_5Me_5)B_4H_{11}]$ whilst $[Ru(\eta\text{-}C_5Me_5)H_2]_2$ gives the bimetallaborane cluster *nido*-1,2-$[\{Ru(\eta\text{-}C_5Me_5)\text{-}H\}_2B_3H_7]$ which reacts further with $BH_3 \cdot$ thf to give *nido*-1,2-$[\{Ru(\eta\text{-}C_5Me_5)\}_2(\mu\text{-}H)B_4H_9]$ [21,22]. More importantly to the present study, reaction of $[W(PMe_3)_3H_6]$ with $BH_3 \cdot$ thf gives a 90% yield of *arachno*-2-$[W(PMe_3)H_3B_3H_8]$ [9]. We sought to access the molybdenum analogue of this tungsten complex using $[Mo(PMe_3)_4H_4]$.

Reaction of $[Mo(PMe_3)_4H_4]$ with one equivalent of $BH_3 \cdot$ thf gives the known borohydride $[Mo(PMe_3)_4H(\eta^2\text{-}BH_4)]$ (**7**) as purple crystals in almost quantitative yield as characterised by NMR spectroscopy [23]. No further reaction ensued with excess $BH_3 \cdot$ thf, even with prolonged heating or UV irradiation.

The difference in reactivity to $BH_3 \cdot$ thf between the tungsten and molybdenum systems may be due to initial dissociation to different 16-electron intermediates. $[W(PMe_3)_3H_6]$ loses dihydrogen to form $\{W(PMe_3)_3H_4\}$ as an intermediate species, whereas $[Mo(PMe_3)_4H_4]$ also loses dihydrogen but to form $\{Mo(PMe_3)_4H_2\}$ as the intermediate. The 16-electron species $\{Mo(PMe_3)_4H_2\}$ can then add a $\{BH_3\}$ fragment to form the isolated product $[Mo(PMe_3)_4H(\eta^2\text{-}BH_4)]$ (**7**). The species $\{W(PMe_3)_3H_4\}$ adds a $\{BH_3\}$ fragment but reacts further via loss of dihydrogen to eventually form the homologated product *arachno*-2-$[W(PMe_3)\text{-}H_3B_3H_8]$. This pathway is not open to $[Mo(PMe_3)_4H(\eta^2\text{-}BH_4)]$ which does not have two terminal hydrides available for loss as dihydrogen. As with $[Mo(PMe_3)_4H_4]$, loss of PMe_3 from $[Mo(PMe_3)_4H(\eta^2\text{-}BH_4)]$ is not a favoured dissociative pathway.

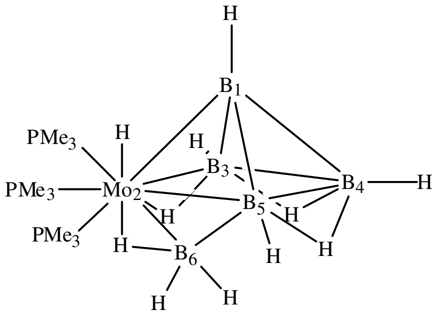

Fig. 7. Proposed structure for *nido*-2-$[Mo(PMe_3)_3HB_5H_{10}]$ (**6**).

3. Conclusions

Reaction of pentaborane(9) with electron-rich Group 6 metal phosphine polyhydride complexes gives two classes of metallaboranes which have been characterised. The first structural class contains the well-known nido-"MB_4H_8" cluster. The second class represented by *nido*-2-$[W(PMe_2Ph)_3HB_5H_{10}]$ (**2**) has a novel metallaborane structure containing an edge-bridging $\{BH_3\}$ group between the tungsten atom and one of the basal boron atoms in a "*nido*-WB_4" pyramid.

4. General methods and instrumentation

All preparations, manipulations and reactions were carried out under an inert atmosphere of dinitrogen using standard techniques for handling air-sensitive materials (Schlenk line and glove-box). Dinitrogen was purified by passage through a column containing BASF catalyst and 4 Å molecular sieves. Solvents were pre-dried over molecular sieves (4 or 5 Å), distilled from appropriate drying agents and stored under dinitrogen in Teflon valve ampoules. Deuterated solvents were stored over activated molecular sieves or sodium-potassium alloy. Chromatography was carried out on silica gel G (Fluka, type GF 254) under dinitrogen. Reaction mixtures were generally deposited as a "sand" on silica gel and admitted to the top of the column via a tipper tube under a gentle stream of dinitrogen. Solvents used for chromatography (thf, petroleum ether and diethyl ether) were not pre-dried but only flushed with dinitrogen before use. Pentaborane(9) was used from stock as a 0.25–0.4 M solution in toluene. $[W(PMe_2Ph)_3H_6]$ [18], $[W(PMe_3)_4(CH_2PMe_2)H]$ [19] and $[Mo(L)_4H_4]$ [20] (L = PMe_3, PMe_2Ph) were prepared according to literature methods. The NMR spectra were obtained using Bruker AM-250 or AM-300 instruments. ^{1}H spectra were referenced internally with respect to the residual protiosolvent (C_6D_6, δ 7.10); ^{11}B and ^{31}P spectra were referenced internally relative to the deuterium lock signal using the SR command of standard Bruker software, with respect to the standards 85% H_3PO_4–D_2O (^{31}P) and BF_3–Et_2O (^{11}B). All chemical shifts are quoted in δ (ppm) and coupling constants in Hertz

(Hz). Mass spectra were obtained on an AEI MS 302 mass spectrometer, "updated" by a data handling system supplied by Mass Spectrometry Services Ltd., (EI or FAB) by the SERC Mass Spectrometry Centre at the University College of Swansea. Elemental analysis was carried out by the analysis department of the Inorganic Chemistry Laboratory, Oxford University.

4.1. X-ray structure determinations

Data were collected on an Enraf.Nonius CAD4 diffractometer ($3^\circ > 2\theta < 50^\circ$). The structure was solved from direct methods and Fourier syntheses and refined by full-matrix least-squares procedures with anisotropic thermal parameters for all non-hydrogen atoms. Hydrogen atoms bonded to carbon atoms were included in calculated positions (C–H 0.96 Å) and refined riding on their attached atom. Hydrogen atoms bonded to boron atoms were located from a difference synthesis and their co-ordinates and isotropic thermal parameters refined. Crystallographic calculations were carried out using the Oxford "CRYSTALS" package [24].

4.1.1. Reaction of [$W(PMe_2Ph)_3H_6$] with pentaborane(9)

[$W(PMe_2Ph)_3H_6$] (1.2 g, 2.00 mmol) in toluene (40 ml) was treated with a toluene solution of pentaborane(9) (0.404 M, 20 ml). The orange solution was left stirring at ambient temperature for 18 h during which time it had changed to a red–brown colour. The reaction mixture was then chromatographed on a silica gel column. Light petroleum ether:thf 20:1 eluted *nido*-2-[$W(PMe_2Ph)_3H_2B_4H_8$] (**1**) as a bright yellow band. Light petroleum ether:thf 9:1 eluted [$W(PMe_2Ph)_3HB_5H_{10}$] (**1**) as a dark orange–brown band. Recrystallisation of the yellow band from light petroleum ether afforded yellow microcrystals of (**1**), yield 70 mg, 5%. The orange–brown band was recrystallised from toluene:light petroleum ether 1:1 to give purple needles of (**2**) suitable for X-ray diffraction, yield 130 mg, 10%.

Compound (**1**). Elemental analysis for $C_{24}H_{43}B_4WP_3$. Anal. Calc.: C, 44.2; H, 6.6. Found: C, 44.3; H, 6.9%.

Selected NMR data: $^1H\{^{11}B\}$ NMR (toluene-d_8): $\delta = 7.2$ [br m, 1H, 3Ph], 5.2 [s, 1H, H(4)], 3.4 [s, 2H, H(3) and H(5)], 1.5 [d, 18H, *J*(P–H) 8, 3 PMe_2], 1.1 [s, 1H, H(1)], −2.2 [s, 2H, H(34) and H(45)], −3.3 [q, 2H, *J*(P–H) 43, 2W–H], −8.5 [s, 2H, H(23) and H(25)]. ^{11}B (benzene-d_6): δ −3.1 [br d, 1B, *J*(B–H) 138, B(4)], −9.3 [br s, 2B, B(3) and B(5)], −28.8 [d, 1B, *J*(B–H) 148, B(1)].

Compound (**2**). Mass spectrum: $m/z = 686$, $[M + Na]^+$. Elemental analysis for $C_{24}H_{44}B_5WP_3$. Anal. Calc.: C, 43.5; H, 6.7. Found: C, 44.4; H, 7.4%.

Selected NMR data: $^1H\{^{11}B\}$ NMR (toluene-d_8): $\delta = 7.1$ [s, 2H, H(6) and H(7)], 7.0 [m, 15H, 3Ph], 5.7 [s, 1H, H(4)], 4.0 [s, 1H, H(3)], 3.1 [s, 1H, H(1)], 1.8 [s, 1H, H(5)], 1.7 [d, 3H, *J*(P–H) 9, PMe], 1.6 [d, 3H, *J*(P–H) 8, PMe], 1.5 [d, 3H, *J*(P–H) 8, PMe], 1.5 [d, 3H, *J*(P–H) 8, PMe], 0.9 [d, 3H, *J*(P–H) 8, PMe], 0.9 [d, 3H, *J*(P–H) 7, PMe], 0.3 [br m, 1H, W–H], −1.5 [s, 1H, H(34)], −4.4 [s, 1H, H(45)], −6.8 [m, 1H, H(23)], −10.7 [m, 1H, H(26)]. ^{11}B (benzene-d_6): δ 32.0 [br t, 1B, B(6)], 11.0 [d, 1B, *J*(B–H) 122, B(4)], 6.83 [d, 1B, *J*(B–H) 153, B(1)], −4.7 [br d, 1B, *J*(B–H) 122, B(3)], −10.7 [d, 1B, *J*(B–H) 134, B(5)]. $^{31}P\{^1H\}$(benzene-d_6): −16.7 [d, 2P, *J*(P–P) 10], −29.3 [t, 1P, *J*(P–P) 9].

4.2. Reaction of [$W(PMe_3)_4(\eta^2\text{-}CH_2PMe_2)H$] with pentaborane(9)

A solution of pentaborane(9) in toluene (0.15 M, 30 ml) was added to a solution of [$W(PMe_3)_4(\eta^2\text{-}CH_2PMe_2)H$] (1.0 g, 1.8 mmol) in toluene (50 ml) and stirred at ambient temperature for 3 days. The yellow solution darkened considerably. The reaction mixture was then chromatographed on a silica gel column eluting with light petroleum ether:thf 9:1. Four bands separated which were yellow, orange, purple and brown–purple. Band 1 was recrystallised from petroleum ether to give *nido*-2-[$W(PMe_3)_3H_2B_4H_8$] (**3**) as yellow crystals, yield 40 mg, 5%. The other bands were obtained in insufficient quantity for full characterisation, although the purple band was studied by multi-nuclear NMR.

Compound (**3**). Elemental analysis for $C_9H_{37}B_4WP_3$. Anal. Calc.: C, 22.93; H, 8.07. Found: C, 22.83; H, 8.34%.

Selected NMR data: $^1H\{^{11}B\}$ NMR (benzene-d_6): $\delta = 5.36$ [s, 1H, H(4)], 3.5 [s, 2H, H(3) and H(5)], 1.4 [d, 27H, *J*(P–H) 7, 3 PMe_3], 1.05 [s, 1H, H(1)], −2.1 [s, 2H, H(34) and H(45)], −4.05 [q, 2H, *J*(P–H) 39, 2W–H], −8.75 [s, 2H, H(23) and H(25)]. ^{11}B: δ −3.66 [br d, 1B, *J*(B–H) 138, B(4)], −9.72 [br d, 2B, *J*(B–H) 105, B(3) and B(5)], −29.75 [d, 1B, *J*(B–H) 157, B(1)]. $^{31}P\{^1H\}$: −28.7 [s, 3PMe_3).

4.3. Reaction of [$Mo(PMe_3)_4H_4$] with pentaborane(9)

A solution of pentaborane(9) in toluene (0.41 M, 25 ml) was added to a solution of [$Mo(PMe_3)_4H_4$] (2 g, 5.0 mmol) in light petroleum (20 ml) and the solution stirred at ambient temperature for 16 h. The dark red–brown solution deposited some brown solids. The reaction mixture was chromatographed on silica gel eluting with light petroleum:diethyl ether 20:1. A yellow band was eluted and collected. Recrystallisation from light petroleum ether at −30 °C gave yellow brick-shaped crystals of *nido*-2-[$Mo(PMe_3)_3H_2B_4H_8$] (**4**), yield 0.18 g, 10%.

Compound (**4**). Elemental analysis for $C_9H_{37}B_4MoP_3$. Anal. Calc.: C, 28.6; H, 9.9. Found: C, 28.4; H, 10.2%.

Selected NMR data: $^1H\{^{11}B\}$ NMR (benzene-d_6): $\delta = 3.92$ [s, 1H, H(4)], 3.14 [s, 2H, H(3) and H(5)], 1.23 [virt. t, 27H, 3 PMe_3], 1.08 [s, 1H, H(1)], −2.03 [s, 2H, H(34) and H(45)], −4.53 [q, 2H, *J*(P–H) 47, 2Mo–H], −8.85 [s, 2H, H(23) and H(25)]. ^{11}B: δ −2.64 [d, 1B, *J*(B–H) 134, B(4)], −7.32 [d, 2B, *J*(B–H) 150, B(3) and B(5)], −27.20 [d, 1B, *J*(B–H) 150, B(1)]. $^{31}P\{^1H\}$: 8.75 [s, 3PMe_3).

Compound (**6**). Partial NMR data: $^{1}H\{^{11}B\}$ NMR (benzene-d_6): $\delta = -1.1$ [br s, 1H,], −2.6 [dddd, 1H, Mo–H], −3.1 [br s, 1H], −6.4 [br s, 1H], −10.9 [br s, 1H]. ^{11}B: δ 36.6 [br tr., 1B], 13.6 [d, 1B], 10.0 [d, 1B], −4.6 [d, 1B], −6.3 [d, 1B].

4.4. Reaction of [Mo(PMe$_2$Ph)$_4$H$_4$] with pentaborane(9)

A solution of pentaborane(9) in toluene (0.41 M, 15 ml) was added to a solution of [$Mo(PMe_2Ph)_4H_4$] (2 g, 3.1 mmol) in light petroleum (20 ml) and the solution stirred at ambient temperature for 56 h. The reaction mixture was chromatographed on silica gel eluting with light petroleum:diethyl ether 20:1. An orange band was eluted and collected. Recrystallisation from light petroleum ether at −78 °C gave orange–red crystals of *nido*-2-[$Mo(PMe_2Ph)_3H_2B_4H_8$] (**5**), yield 0.08 g, 5%.

Compound (**5**). Elemental analysis (%) of $C_{24}H_{43}B_4MoP_3$. A single analysis of air-sensitive (**5**) was low for both C and H by ca. 6%.

Selected NMR data: $^{1}H\{^{11}B\}$ NMR (benzene-d_6): $\delta = 7.50 - 7.06$ [m, 15H, 3Ph], 4.02 [s, 1H, H(4)], 3.27 [s, 2H, H(3) and H(5)], 1.37 [virt. t, 18H, 3 PMe_2], 1.09 [s, 1H, H(1)], −1.87 [s, 2H, H(34) and H(45)], −3.82 [q, 2H, *J*(P–H) 45, 2Mo–H], −8.51 [s, 2H, H(23) and H(25)]. ^{11}B: δ −2.30 [br s, 1B, B(4)], −7.0 [br s, 2B, B(3) and B(5)], −26.26 [d, 1B, *J*(B–H) 150, B(1)]. $^{31}P\{^{1}H\}$: 21.72 [s, 3PMe_2Ph).

5. Supplementary data

CCDC No. 290788 contains the supplementary crystallographic data for this paper. The data can be obtained free of charge via www.ccdc.cam.ac.uk/conts/retrieving.html (or from the Cambridge Crystallographic Data Centre, 12 Union Road, Cambridge, CB2 1EZ, UK; fax: +44 1223 336 033; or email: deposit@ccdc.cam.ac.uk).

References

[1] L. Barton, Comprehensive Organometallic Chemistry II, Oxford, Pergamon, 1995 (chapter 8).

[2] J.D. Kennedy, Prog. Inorg. Chem. 32 (1984) 519.

[3] J.D. Kennedy, Prog. Inorg. Chem. 34 (1986) 211.

[4] T.P. Fehlner, Organometallics 19 (2000) 2643.

[5] P.D. Grebenik, M.L.H. Green, M.A. Kelland, J.B. Leach, P. Mountford, New J. Chem. 16 (1992) 19.

[6] P.D. Grebenik, M.L.H. Green, M.A. Kelland, J.B. Leach, P. Mountford, J. Chem. Soc., Chem. Commun. (1990) 1234.

[7] M.L.H. Green, J.B. Leach, M.A. Kelland, J. Organomet. Chem. 690 (2005) 4203.

[8] H.J. Bullick, P.D. Grebenik, M.L.H. Green, A.K. Hughes, J.B. Leach, P. Mountford, J. Chem. Soc., Dalton Trans. (1994) 3337.

[9] P.D. Grebenik, J.B. Leach, M.L.H. Green, N.M. Walker, J. Organomet. Chem. 345 (1988) C31.

[10] M.A. Beckett, N.N. Greenwood, J.D. Kennedy, M. Thornton-Pett., J. Chem. Soc., Dalton Trans. (1986) 795.

[11] S. Aldridge, H. Hashimoto, M. Shang, T.P. Fehlner, J. Chem. Soc., Chem. Commun. (1998) 207.

[12] A.S. Weller, M. Shang, T.P. Fehlner, Organometallics 18 (1999) 53.

[13] L.G. Sneddon, D. Voet, J. Chem. Soc., Chem. Commun. (1976) 118.

[14] K. Wade, Adv. Inorg, Chem. Radiochem. 18 (1976) 1.

[15] R.E. Williams, Adv. Inorg, Chem. Radiochem. 18 (1976) 67.

[16] D.M.P. Mingos, Nat., Phys. Sci. 236 (1972) 99.

[17] R. Greatrex, N.N. Greenwood, M.B. Millikan, D.W.H. Rankin, H.E. Robertson, J. Chem. Soc., Dalton Trans. (1988) 2335.

[18] J.R. Moss, B.L. Shaw, J. Chem. Soc., Dalton Trans. (1972) 1910.

[19] V.G. Gibson, P.D. Grebenik, M.L.H. Green, J. Chem. Soc., Chem. Commun. (1983) 1101.

[20] D. Lyons, G. Wilkinson, J. Chem. Soc., Dalton Trans. (1985) 587.

[21] M.A. Peldo, A.M. Beatty, T.P. Fehlner, Organometallics 21 (2002) 2821.

[22] M.A. Peldo, A.M. Beatty, T.P. Fehlner, Organometallics 22 (2003) 3698.

[23] J.L. Attwood, W.E. Hunter, E. Carmona-Guizman, G. Wilkinson, J. Chem. Soc., Dalton Trans. (1980) 467.

[24] D.J. Watkin, J.R. Carruthers, P. Betterridge, CRYSTALS User Guide, Chemical Crystallography Laboratory, University of Oxford, Oxford, 1985.

[25] H.J. Bullick, P.D. Grebenik, M.L.H. Green, A.K. Hughes, J.B. Leach, P.C. McGowan, J. Chem. Soc., Dalton Trans. (1995) 67.